RSC Advances

ROYAL SOCIETY OF CHEMISTRY

www.rsc.org/advances

Contents entry

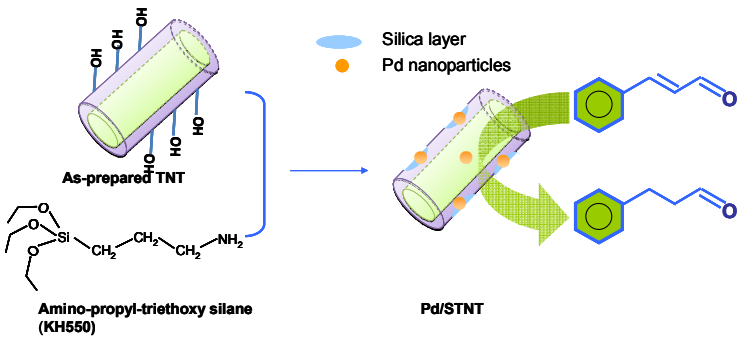

- A Pd/STNT catalyst, with silica modified titanate nanotubes as support, exhibited significantly enhanced activity towards hydrogenation of cinnamaldehyde.

Figure and Tables Captions

Table 1 Specification of various support and catalysts.

Table 2 XPS data: binding energy and atomic ratio of various Pd catalysts.

Table 3 Hydrogenation of CALD over various catalysts: mass reaction rate and product selectivity.

Scheme 1 Preparation route of silica modified TNT (STNT) and Pd/STNT catalyst

Fig. 1 XRD patterns of various catalysts and support.

Fig. 2 Raman spectra of various catalysts

Fig. 3 TEM images of as-prepared TNT (a-b), Pd/TNT (c-d), and Pd/STNT (e-f).

Fig. 4 XPS spectra of catalysts

Fig. 5 H_2-TPD pattern of various catalysts

Fig. 6 Reaction pathway for the hydrogenation of CALD over Pd catalyst

Fig. 7 Course of hydrogenation of CALD over a) Pd/TNT and b) Pd/STNT.

Tables

Table 1 Specification of various support and catalysts.

Sample	S_{BET} (m^2 g^{-1})	$D_{inner\ pore}$ (nm)	TiO_2 Crystal. size (nm)	Pd *wt.%*	Pd crystal. size (nm)
as-prepared TNT	302	8.0	-	-	-
Pd/TNT	145	3.3	8.5	2.5	6.2
Pd/STNT	270	7.0	7.1	2.4	4.5

Table 2 XPS data: binding energy and atomic ratio of various Pd catalysts.

Catalyst	Binding energy (eV)			Atomic ratio	
	$Pd^0{}_{3d5}$	$Pd^{II}{}_{3d5}$	Ti_{2p3}	Pd/Ti	Pd^0/Pd^{II}
[a] Pd/C	335.1	336.5	-	-	-
Pd/TNT	335.5	336.9	458.4	0.06	0.54
Pd/STNT	335.9	337.2	458.6	0.05	0.81

[a] data in our previous reported document[37]

Table 3 Hydrogenation of CALD over various catalysts: mass reaction rate and product selectivity.

Catalyst	r (g_{CALD} g_{Pd}^{-1} h^{-1})	Selectivity (%)[b]		
		HALD	HALC	CALC
[a] Pd/C	48	87	12	<1
Pd/TNT	65	85	14	1
Pd/STNT^{1st}	151	84	15	1
Pd/STNT^{3rd}	137	82	16	2

[a] commercial Pd/C catalysts bought from Aladin agent company (Shanghai, China)

[b] Selectivity was determined at 80% CALD conversion; no other product was found in the GC-mass spectra.

Scheme and Figures

Scheme 1

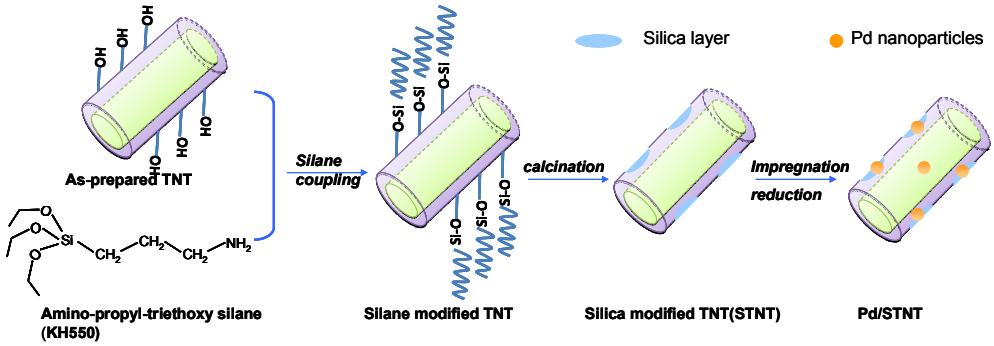

Scheme 1 Preparation route of silica modified TNT (STNT) and Pd/STNT catalyst

Fig.1

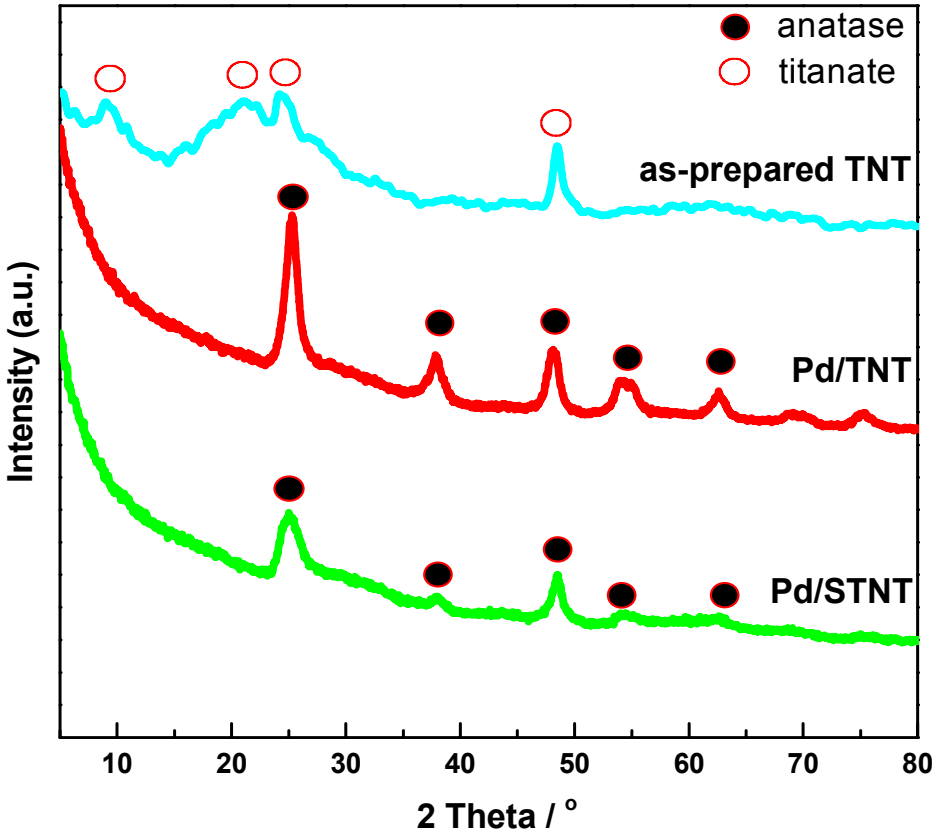

Fig. 1 XRD patterns of various catalysts and support

Fig.2

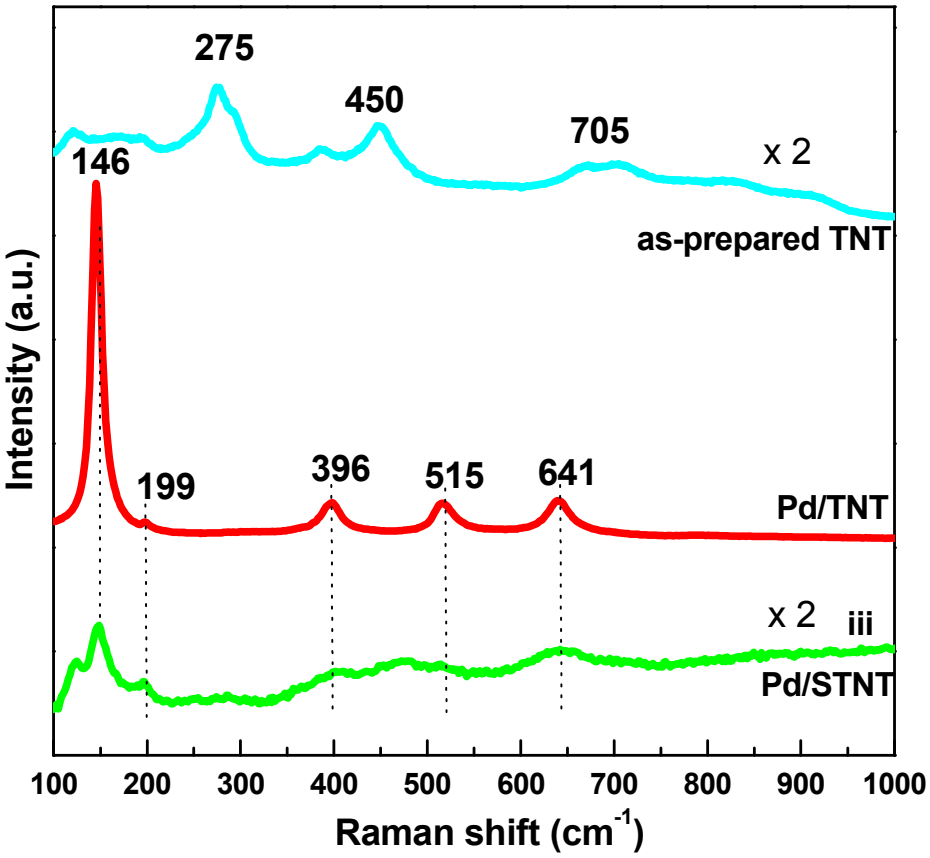

Fig. 2 Raman spectra of various catalysts

Fig.3

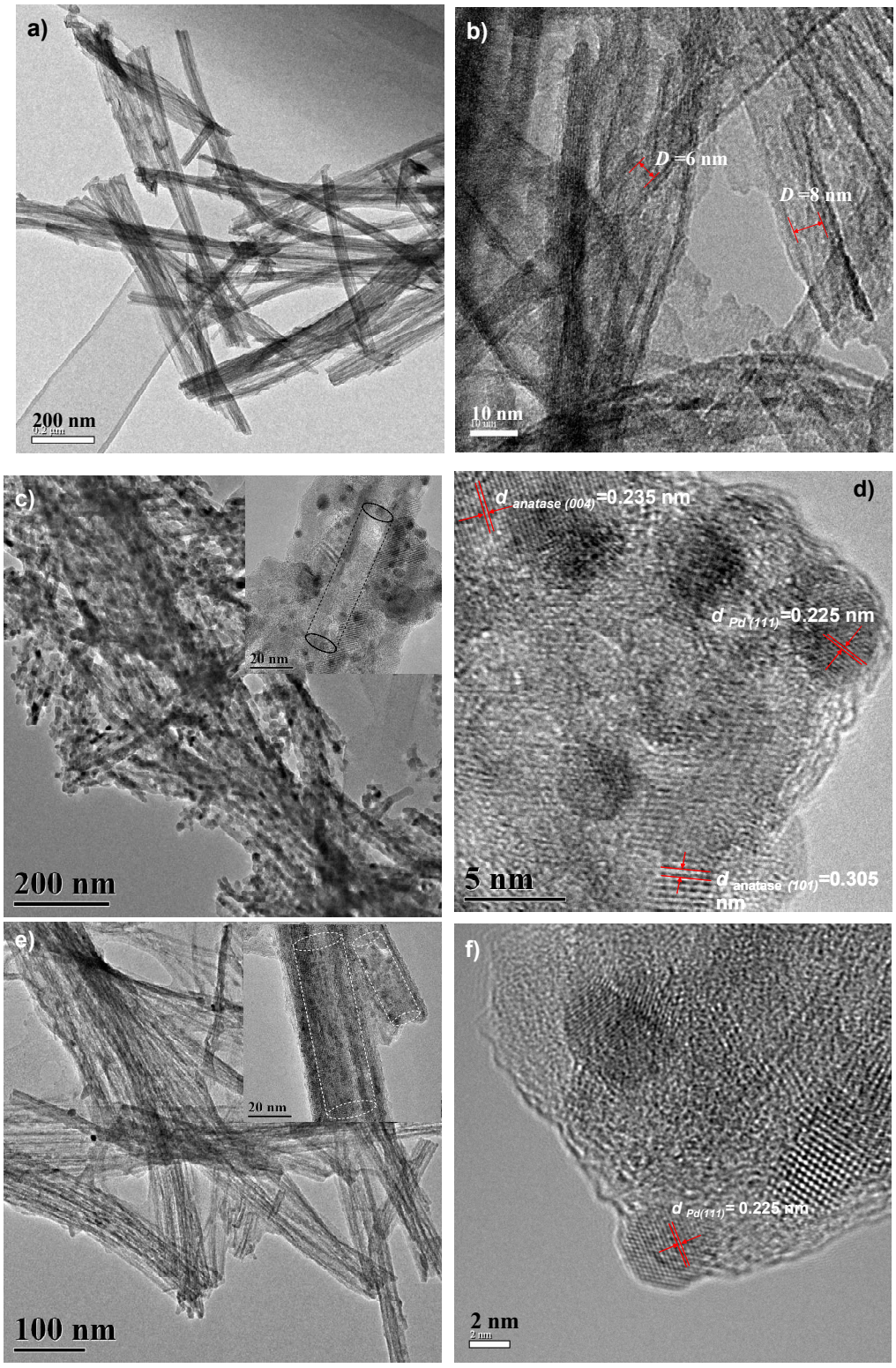

Fig.4

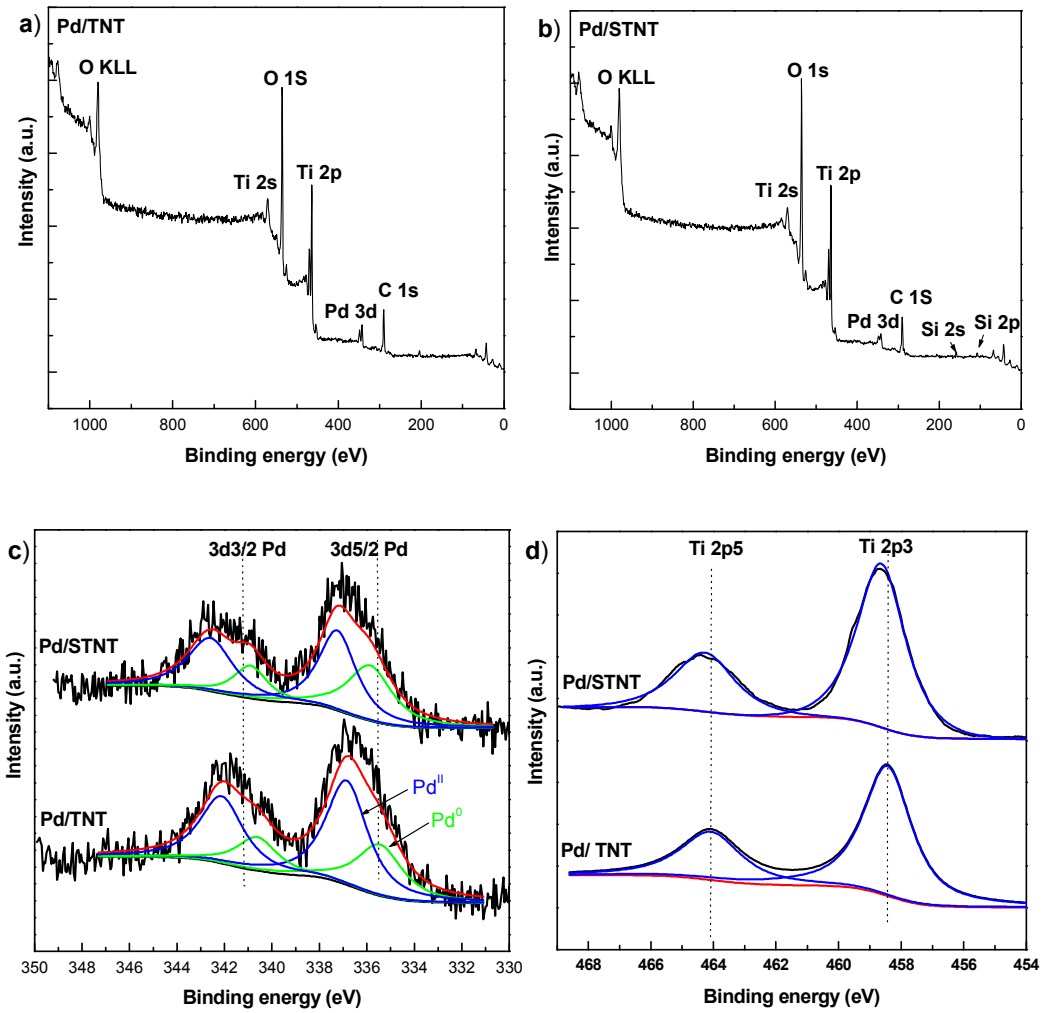

Fig. 4 XPS spectra of catalysts

Fig.5

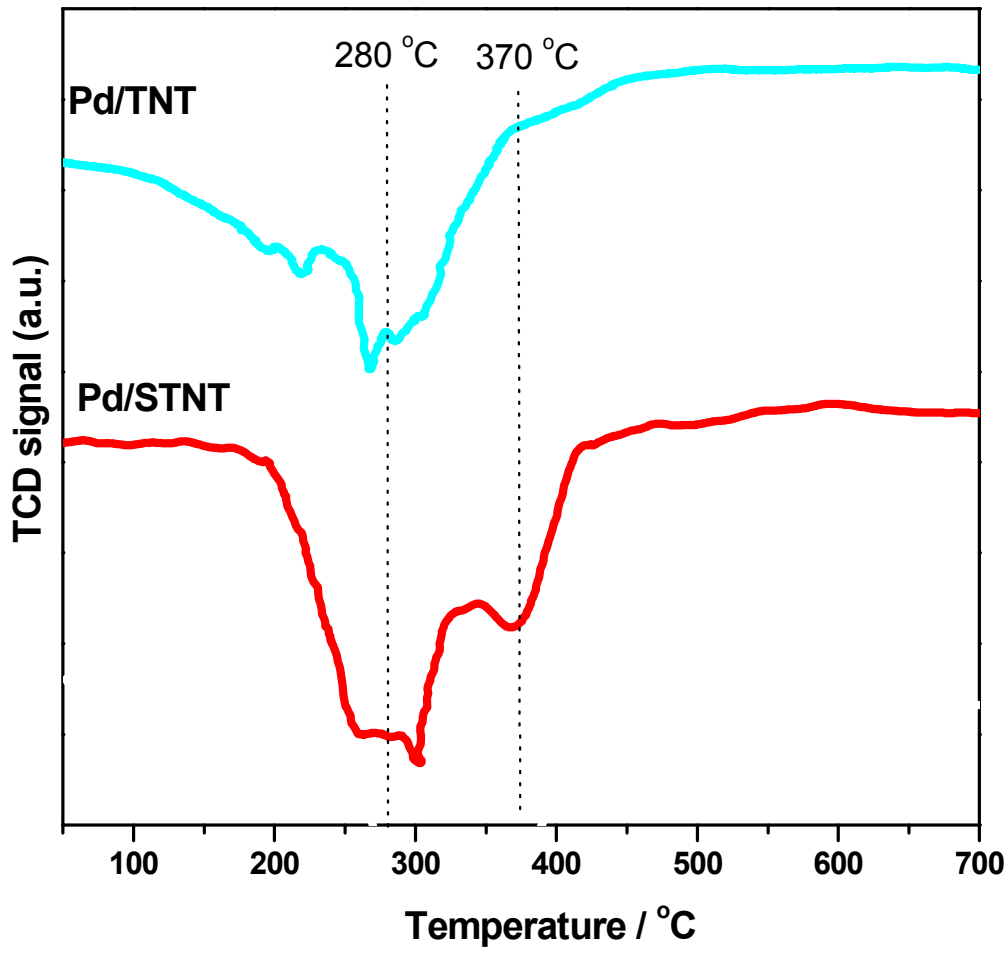

Fig. 5 H_2-TPD pattern of various catalysts

Fig.6

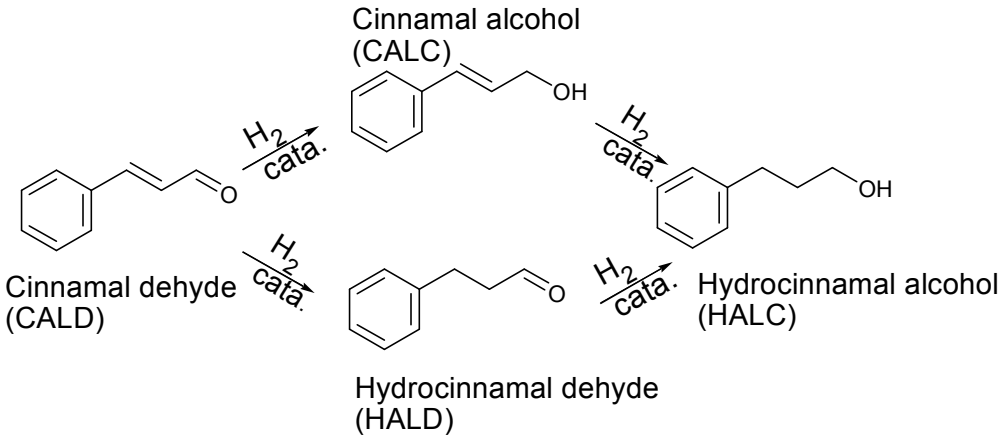

Fig. 6 Reaction pathway for the hydrogenation of CALD over Pd catalyst

Fig.7

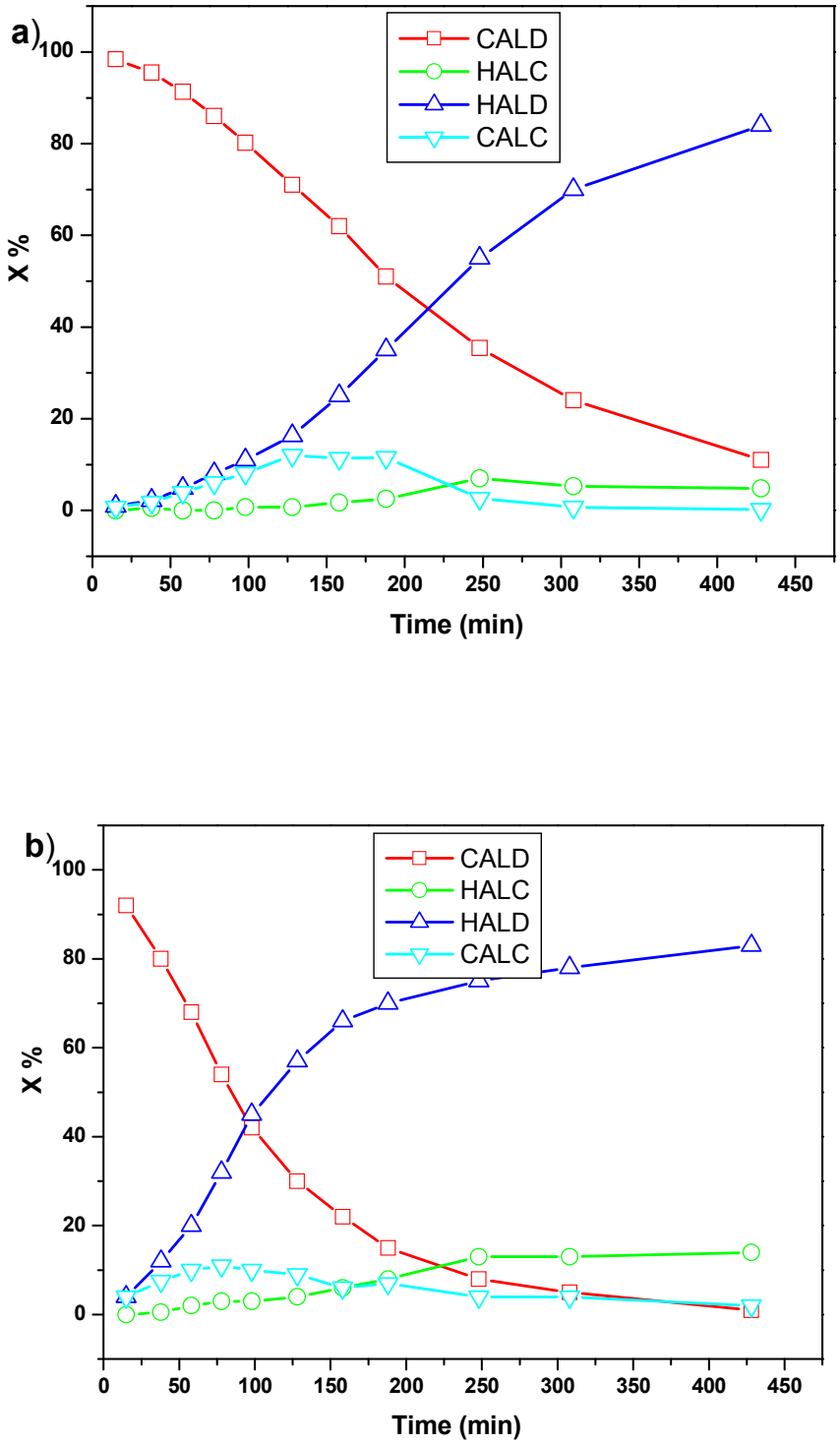

Fig. 7 Course of hydrogenation of CALD over a) Pd/TNT and b) Pd/STNT.

Cite this: DOI: 10.1039/c0xx00000x

www.rsc.org/xxxxxx

ARTICLE TYPE

High performance Pd catalyst using silica modified titanate nanotubes (STNT) as support and its catalysis toward hydrogenation of cinnamaldehyde at ambient temperature

Xu Yang[a], Liangpeng Wu[a], Li Du[b], Lizhen Long[a],Tiejun Wang[a], Longlong Ma[a], Xinjun Li*[a], Shijun Liao*[b]

Received (in XXX, XXX) XthXXXXXXXXX 20XX, Accepted Xth XXXXXXXXX 20XX
DOI: 10.1039/b000000x

Titanate nanotubes (TNT) were coupled with amino-propyl-triethoxysilane (KH550) and calcinated at 400 °C, then the silica modified titanate nanotubes (STNT) were prepared and used as support of Pd catalyst by method of wet-impregnation. The catalysts were characterized with XRD, Raman spectra, TEM, XPS, and H_2-TPR/TPD. The silica modification could effectively resist morphology collapse and crystallization of TNT during calcination, and preserve the high surface area of TNT support, which contribute to the high metal dispersion of loaded Pd. Moreover, the introduced silica could strengthen the metal-support interaction, cause electronic effect that facilitates the reduction of Pd ions. The Pd/STNT showed 3 times and 2.5 times higher activity than that of commercial Pd/C and unmodified Pd/TNT catalysts towards the selective hydrogenation of cinnamaldehyde at room temperature, respectively, indicating well the enhanced catalytic activity by addition of silica.

1.Introduction

Growing concern about energy availability and related environmental impacts has in recent years led many scientists to investigate*green catalysis*, which requires chemical transformations to be catalyzed using clean,efficient methods and materials[1-7]. One effective strategy to achieve this target is to develop high-performance heterogeneous catalysts for useat room temperature.

To date, many investigations in the field of heterogeneous catalysis have revealed that the microstructure/composition of the loaded active components is closely related to the physico-chemical properties of the supports (surface chemistry, surface area, crystallinity, morphology, etc.). The interaction between metal and support, an important factor influencing the catalysis process, is also strongly associated with the support's surface physical-chemical properties. Considerable work on various support modifications has been done to fine-tune the general properties of the support. For example, multiple inorganic oxide composites, such as NiO-TiO_2[8, 9], Carbon-Titania[10], TiO_2-SiO_2[11, 12], and Al_2O_3-TiO_2[11, 13, 14], have been used as supports for metal catalysts to obtain a variety of catalytic properties. Adjusting the physico-chemical properties of the support is regarded as an effective method to modulate the catalytic performance of heterogeneous catalysts.

The discovery[15] of titanate nanotubes(TNT) has attracted significant attention because of their many advantages, including their tubular morphology, and modest cost. TNT is an excellent support material for heterogeneous catalysis becauseit can effectively improve the dispersion of theloaded metal, a feature attributable to its tubular structureand large surface area[16-18]. Furthermore, the abundant –OH groups on the surface of TNT facilitate the introduction of inorgnaic/organic molecule to modify that surface with various structure and composition. Recently, researchers have demonstrated that TiO_2 surface structure and properties, such as surface potential[19], and crystalline degree[20], can be tuned effectively by the addition of silica, which could change the TNT's surface composition, influence the interface interaction between the TNT and the loaded components and yieldvarious catalytic properties. More importantly, the deposited silica could act as "isolated layer", a feature widely applied in constructing metal core-silica shell nanocomposites[21-24]. Thus, supposed that it may protect the TNT's multiple wall from damage, which often occurres at calcination larger than 400 °C and would limit its practical application in the heterogeneous catalysis.

Herein, we describeda novel preparation of silica-modified Pd/TNT catalysts by modifying the TNT surface with amino-propyl-triethoxysilane (KH550), then using the silane/silica-modified TNT as the catalyst support. To the best of our knowledge, there is no literature involving with silica modified TNT as support of Pd catalyst via route of silane modification. This modified catalyst exhibited greatly enhanced performance towards the selective hydrogenation of cinnamaldehyde. We also characterized the catalysts using XRD, XPS, and other techniques,

and attempted to discover the promotion mechanism of silica.

2. Experimental

2.1 Catalyst preparation

Synthesis of support materials: Titanate nanotubes (TNT) were synthesized by a route described in reference [15]. As-received TiO_2 (Hualisen Corp., China) was mixed with 100 mL concentrated NaOH solution (10M) and placed in a Teflon-lined autoclave under mild stirring at 140 ℃ for 24 h, then the resultant white precipitate was separated from the mixture and washed with deionized water several times until the conductivity of the solution remained below 100 μscm^{-1}.

Modification of TNT with silica: Amino-propyl-triethoxysilane (KH550)was used as silane couplers (see Scheme 1 for their molecular structures).Modification of TNT was conducted as follows: in a mass ratio of 2:1, pristine TNT and KH550 were added to a water–ethanol mixed solution under vigorous stirring at 50 ℃ for 5 h. The resulting white precipitate was filtered, washed with ethanol to eliminate the extra KH550, and dried at 60 ℃ for overnight. Finally, the silane modified TNT was calcinated in the oven at 400 °C for 3 h to transform into silica modified TNT. We denote the silica modified TNT as STNT.

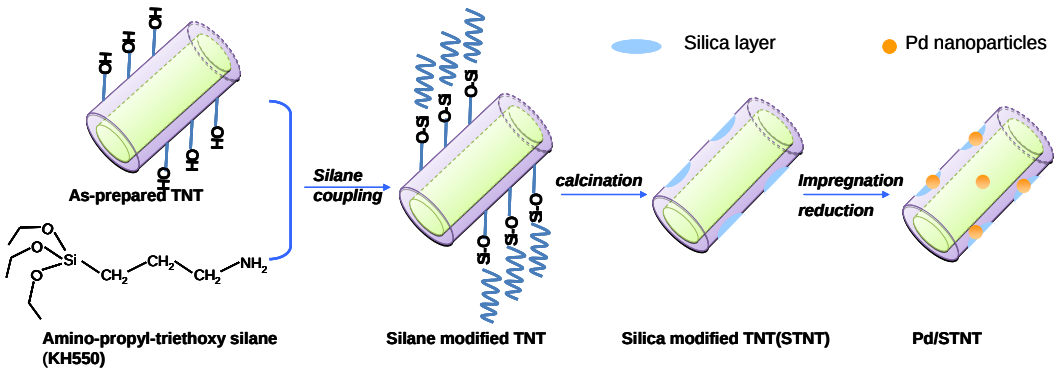

Scheme 1 Preparation route of silica modified TNT (STNT) and Pd/STNT catalyst

Preparation of catalyst: TNT-supported palladium catalysts were prepared by the following procedures. First, the support was impregnated viathe incipient wetness impregnation technique, using an aqueous solution containing a calculated amount of $PdCl_2$; the mixture was then vacuum dried overnight at 40 ℃, followed by calcination in air at 400 ℃ for 2 h. The Pd loading was fixed at ca. 2.5 wt%. These preparation procedures are presented in Scheme 1.

2.2 Catalyst characterization

X-ray diffraction (XRD) patterns were obtained with an X'Pert Pro MPD X-ray diffractometer (PANalytical, Netherlands) using Cu Kα radiation.

Raman measurement was carried out using a Raman spectroscope (HORIBA Jobin Yvon LabRAM HR, France). The power of the laser was 10 mW, and the laser excitation was 488 nm. Scans were taken over an extended range (100–1000 cm^{-1}), and the exposure time was 20 s.

N_2 adsorption-desorption isotherms were measured with a Tristar 3010 isothermal nitrogen sorption analyzer (Micromeritics, USA) using a continuous adsorption procedure.

Transmission electron microscopy (TEM) was carried out on a JEM-2010 microscope (JEOL, Japan) using an accelerating voltage of 200 kV.

X-ray photoelectron spectroscopy (XPS) was performed withan AXIS Ultra DLD (Kratos, Britain) to examine the catalysts' electronic properties. The C 1s line was taken as an internal standard at 284.8eV.

Hydrogen temperature-programmed reduction/desorption (H_2-TPR/TPD) was performed on an Autosorb-iQ-C automated system (Quantachrome, USA). Approximately 50 mg of as-prepared catalyst was placed in a quartz tube within a temperature-controlled oven. H_2-TPR was conducted using a heating rate of ca. 10 ℃ min^{-1} from 35 to 800 ℃. For H_2-TPD, the catalyst was first reduced in H_2 flow at 100 cm^{3}min^{-1} for 1 h at 400 ℃ and then cooled to room temperature. TPD was performed using a constant heating rate of ca. 10 ℃min^{-1} from 35 to 600 ℃.

2.3 Catalyst evaluation

The selective hydrogenation of cinnamaldehyde was used to evaluate the catalysts. The reaction mixture—composed of 0.2 g cinnamaldehyde (CALD), 20 mg catalyst, and 10 mL hexane—was introduced into a stainlesssteel autoclave under stirring at 1200 rpm, a value chosen to eliminate the mass transfer limitation. Air in the autoclave was purged by hydrogen for 20 min, and then the reaction proceeded at room temperature (25 ℃) and 0.5 MPa of 99.99% hydrogen.

The products were analyzed by a gas chromatograph (Agilent 6840N, USA) equipped with a flame ionization detector. Gas chromatography–mass spectrometry(GC-MS) analysis was carried out using a Shimadzu GCMS-QP5050A (Japan) equipped with a 0.25 mm × 30 m DB-WAX capillary column, to identify the product. The column oven temperature was programmed from 120 ℃ (held for 1 min) to 280 ℃ at a rate of 20 ℃min^{-1}.

The mass reaction rate, r, was determine using the equation below:

$$r = \frac{m_{CALD}}{m_{Pd} \times t_{react}}$$

where m_{CALD}, m_{Pd}, and t_{react} stand for the mass of CALD converted, the total mass of Pd used, and the reaction time

(typically fixed at an initial 30 min).

3. Results and analysis

3.1 XRD analysis

As shown in Fig. 1, the as-prepared TNT material exhibits a typical titanate phase, which can be assigned to tri-titanate, $(H, Na)_2Ti_3O_7$[15]. After calcination at 400 ℃, all of the catalysts—with either unmodified Pd/TNT or silica modified Pd/STNT—exhibited a typical anatase TiO_2 structure with space group $I4_1/amd$ (JCPDS card No. 21-1272)[25]. However, the diffraction intensity of the Pd/STNT is clearly much weaker than that of the Pd/TNT, revealing that silica modification obstructed modification to the crystallization of the TNT support. By applying the Scherrer equation to the (101) peak of each support, the crystallite sizes of TNT, and STNT particles were estimated to be 7.9 and 4.5 nm, respectively, further confirming that the presence of silica mayhave affectedthe crystalline degree of TNT during calcination. This result is quite consistent with that reported by Okada et al.[26]who found that the crystallinity of anatase decreased and the crystallization temperature increased upon the addition of silica. It should be pointed out that no obvious diffraction peaks indexed to metallic Pd could be observed in the XRD patterns. There may be two reasons for this:a low supporting amount of Pd (2.5 %), and high dispersion of Pd on the TNT supports[27, 28].

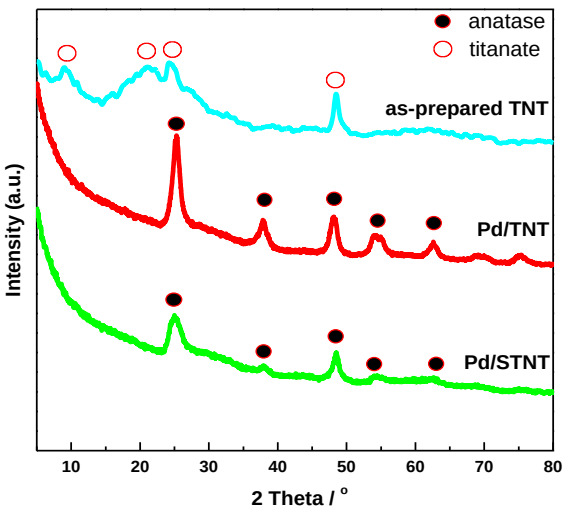

Fig. 1 XRD patterns of various catalysts and support

3.2 Raman spectra analysis

The corresponding Raman spectra of the catalysts are given in Fig. 2.The Raman spectra provide a way to measure the percentage of anatase TiO_2 exposed facets from the micro perspective of molecular bonding. The pattern of the as-prepared TNT (with 2× magnification) shows four well-defined active mode at 275, 385, 450, and 705 cm^{-1}, similar to the spectrum of titanate reported by Gao[29] and Li[15]. After calcination, the Pd/TNT shows spectrum with five sharp contributions at 146, 199, 398, 515, and 641cm^{-1}, in good agreement with the theoretical analysis and the published data[30], indicatingthat the as-prepared TNT were transformed into an anatase-phase TiO_2. The modified Pd/STNT, show peaks (with 2× magnification) similar to but much weaker than those of Pd/TNT. This is a good demonstration that the introduced silica effectively weakened the crystallinity of TNT undergoing calcination, a finding that is consistent with the XRD results.

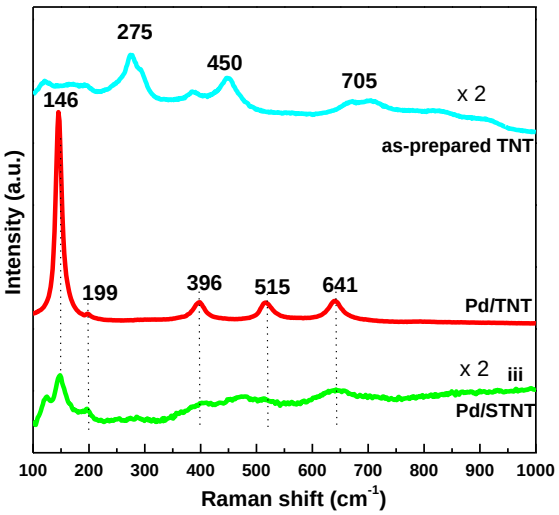

Fig. 2 Raman spectra of various catalysts

3.3 Nitrogen sorption analysis

Table 1 gives the surface areas and porosity parameters of various samples. The as-prepared TNT shows high surface area of 302 m^2/g with meso-pores of 8.0 nm. Undergoing calcination, the surface area of Pd/TNT decreased sharply, with ca. 50% decline, in accordance with previous observation reported by Emorgado et al[31]. While for the Pd/STNT, the surface area and the pore size decreased (by 50% for surface area and ~10% for pore size). These resultsstate that the silica modification could effectively preserve TNT's high surface area undergoing calcination.

Table 1 Specification of various support and catalysts.

Sample	S_{BET} (m^2g^{-1})	$D_{innerpore}$ (nm)	TiO_2Crystal. size (nm)	Pd *wt.%*	Pd crystal. size (nm)
as-prepared TNT	302	8.0	-	-	-
Pd/TNT	145	3.3	8.5	2.5	6.2
Pd/STNT	270	7.0	7.1	2.4	4.5

3.4 TEM observation

Fig. 3 presents TEM images of the samples. The tubular morphology can be seen clearly for the as-prepared TNT, and the inner cavity is 6–8 nm, consistent with the BET results. For the Pd/TNT calcined at 400 °C, it's revealed that in spite of maintaining an elongated feature, some part of the tubular structure collapsed and aggregated to form irregular bulk particles. Similar results have also been reported in documents elsewhere[32, 33]. This result explains well the shrink of surface area for the calcinated TNT. The Pd/STNT treated at 400 °C still exhibited nanotubes features which did not differ from those observed from as-prepared TNT. This result strongly states that the silica modification could improve the thermal stability of TNT, and

preserve well its tubular morphology and high surface area.

As shown in these figures, the Pd dispersion varies. The Pd/TNT presents non-uniform metal dispersion and hasa size range of 4–8 nm; some irregular aggregates as large as 10 nm can be observed as well. The average size of the Pd particles is ca. 7.2 nm. The Pd/STNT catalyst shows a uniformparticle size distribution centered at 4.5 nm. This result indicates that the silica modification can improve the Pd dispersion. A similar finding has been also reported in Binder's work[34], they have ascribed this to the increased surface roughness of support by the addition of silica.

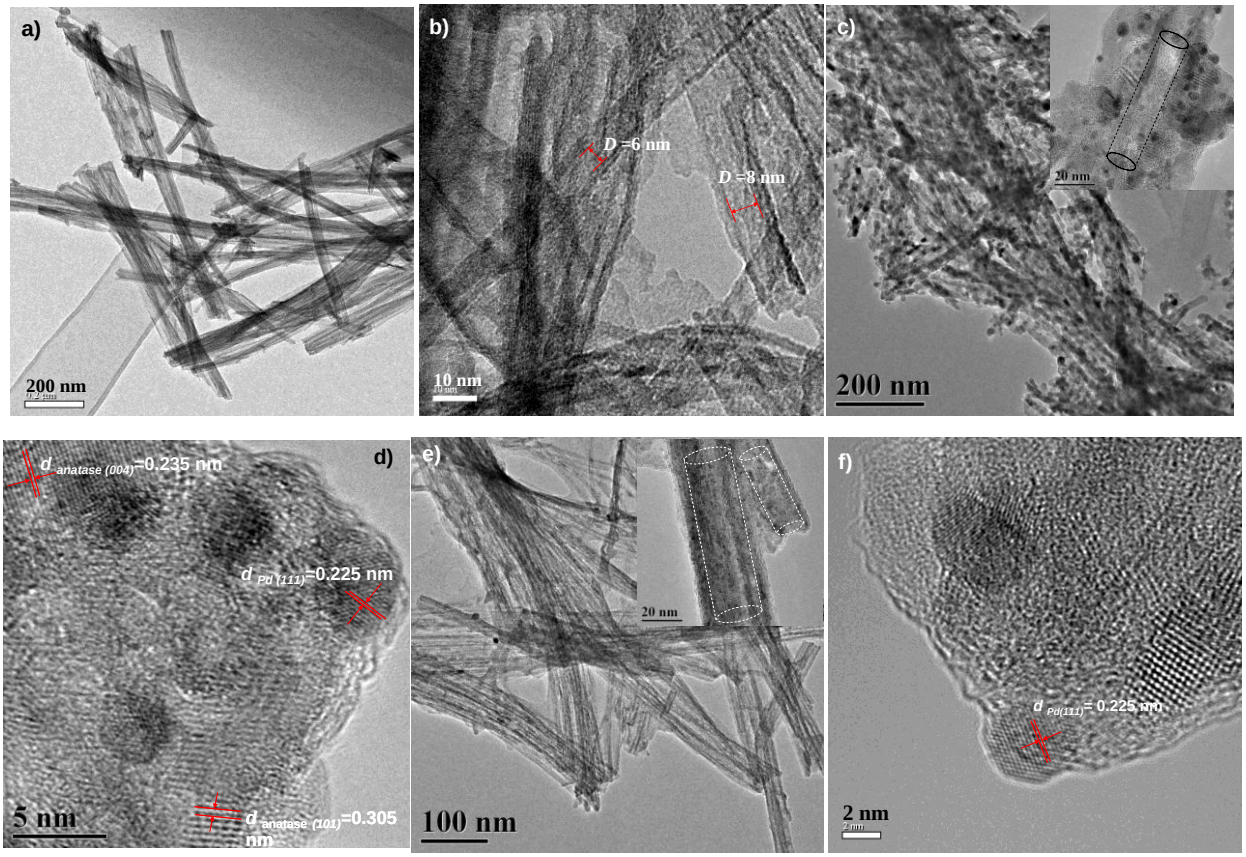

Fig.3 TEM images of as-prepared TNT (a-b), Pd/TNT (c-d), and Pd/STNT (e-f).

3.5 XPS analysis

Fig. 4 shows the XPS spectra of the catalysts. The Pd3d spectra can be deconvoluted into two doublets, attributable to the higher Pd3d energy value of $Pd^{II}O$ and the lower energy value of metallic Pd^0,[35]. A shift of ca. 0.4eV and 0.8 eV toward high binding energy withrespect to the silica-supported mono-Pd catalyst (335.1 eV)[36] can be observed for Pd/TNT and Pd/STNT, respectively, indicating that charge transfer occurred between the Pd and the support. The binding energies centered at ca. 458.6 eV and 102.8 eV correspond to the oxide states of Ti and Si, respectively, confirming the co-presence of titania and silica. Table 2 gives the Pd^0/Pd^{II} ratios; Pd/STNT presents higher value than that of Pd/TNT. This means that the Pd/STNT have higher proportions of metallic Pd than the Pd/TNT, which can be regarded as a result of the electronic effect.

Cite this: DOI: 10.1039/c0xx00000x

www.rsc.org/xxxxxx

ARTICLE TYPE

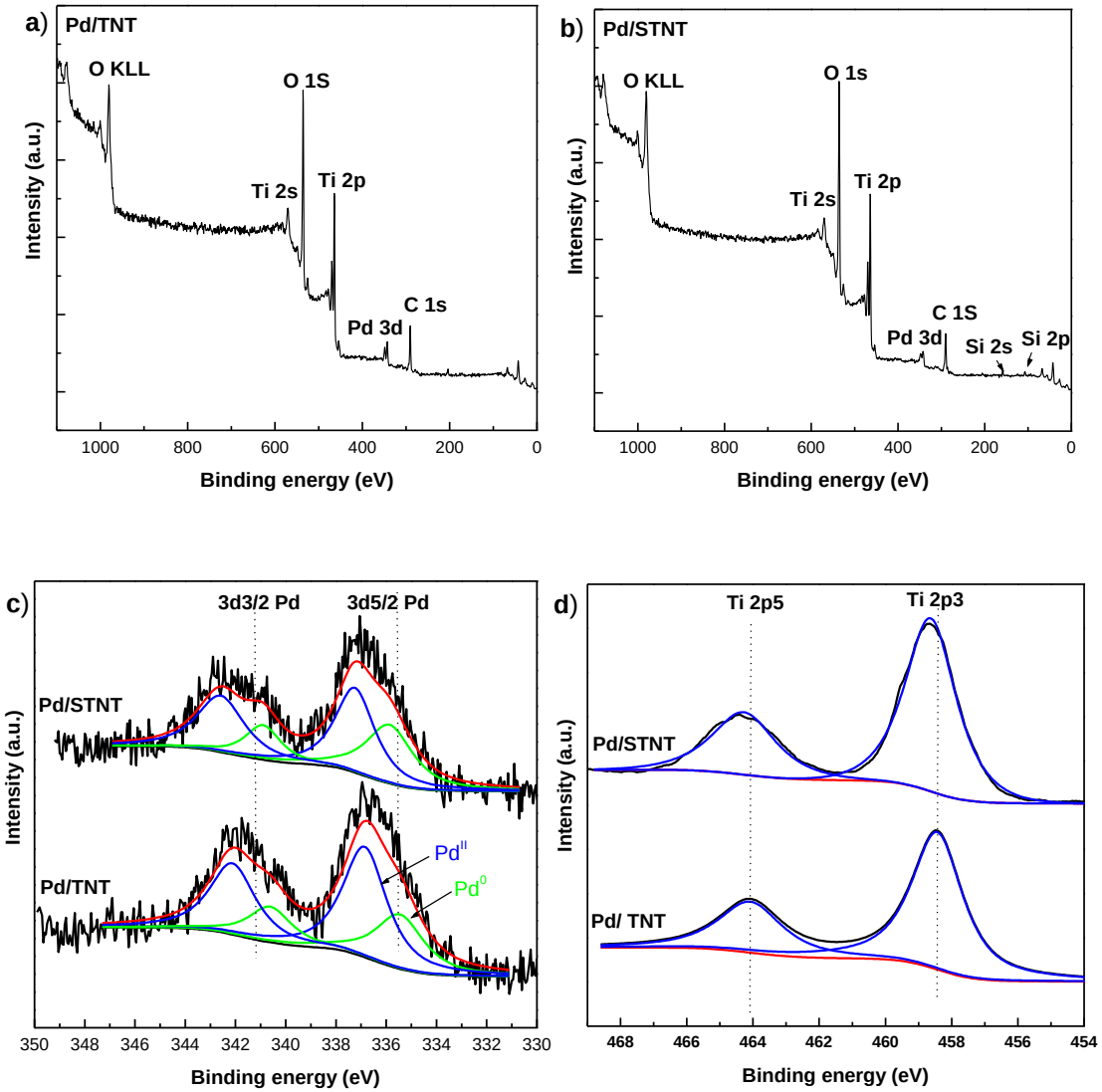

Fig. 4 XPS spectra of catalysts.

Table 2XPS data: binding energy and atomic ratio of various Pd catalysts.

Catalyst	Binding energy (eV)			Atomic ratio	
	Pd^{0}_{3d5}	Pd^{II}_{3d5}	Ti_{2p3}	Pd/Ti	Pd^{0}/Pd^{II}
[a]Pd/C	335.1	336.5	-	-	-
Pd/TNT	335.5	336.9	458.4	0.06	0.54
Pd/STNT	335.9	337.2	458.6	0.05	0.81

[a] data in our previous reported document[37]

3.6 H_2-TPR/TPD analysis

The characteristics of the surface active sites of the catalysts were studied by means of the temperature-programmed reduction/desorption of H_2 (H_2-TPR/TPD) from 50 to 700 °C. No obvious reduction peaks are observable in the TPR patterns of Pd/TNT and, Pd/STNT (not shown for simplicity), implying that most of the Pd^{2+} ions on the support were fully reduced after the H_2/Ar flow was switched into the system at ambient temperature[37].The H_2-TPD profiles of the reduced catalysts are shown in Fig. 5, in which the Pd/TNT and Pd/STNT have two well-defined desorption peaks. Generally, a TPD pattern reveals the various interactions between the adsorbed H_2 species and the Pd particles[38]. By calculating the integrated areas of the H_2 desorption peaks for each catalyst, the H_2adsorption capacities of

Pd/STNT was nearly 2.3 times higher than that of the Pd/TNT. It means that the Pd/STNT possess more active sites than that of the Pd/TNT at ambient temperature.

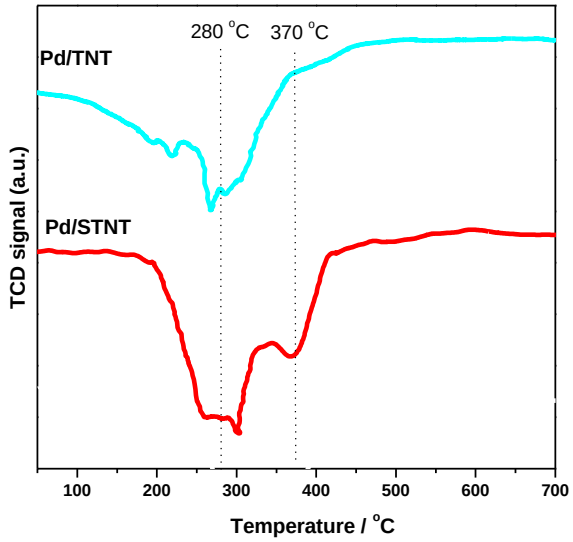

Fig. 5 H_2-TPD pattern of various catalysts

3.7Catalysis towards selective hydrogenation of cinnamaldehyde

The reaction scheme of cinnamaldehyde hydrogenation proceeds via parallel and consecutive pathway that involve with hydrogenation of C=O and C=C groups forming cinnamal alcohol (CALC), hydro-cinnamaldehyde (HALD) and hydrocinnamal alcohol (HALC), seeing Fig. 6.The catalysis of the catalysts towards the hydrogenation of cinnamaldehyde (CALD) was tested under mild reaction conditions (30 ℃ and 0.5MPa of hydrogen pressure).

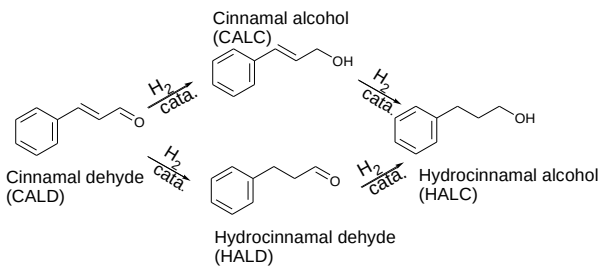

Fig. 6 Reaction pathway for the hydrogenation of CALD over Pd catalyst

As shown in Fig. 7, the introduction of silica seems to have had little effect on the catalysts' product selectivity, which is almost the same for the two catalysts (seeing Table 3).These are common results for Pd catalytic systems, showing that hydrogenation occurs mainly on the C=C bond[36, 39], instead of the Pt catalyzed reaction in which the C=O is preferentially hydrogenated[40]. It is worth noting that the silica modification significantly improved the hydrogenation activity of the affected catalysts. Blank tests carried out over the supports alone showed no catalytic activity. Reaction catalyzed by the Pd/STNT proceeded to a conversion of ~80% in 150 min, while merely 40% of conversion is obtained for the Pd/TNT in the same period. The mass reaction rate *(r)* of catalysts calculated at the initial 30 min reaction, exhibited that the Pd/STNT presents 3 time and 2.5 times higher activity than that of commercial Pd/C and Pd/TNT, respectively. After 3 times of recycle utilization, the Pd/STNT showed ~10 % decrease in reaction rate (seeing Table 3), suggesting the good recyclingstability.

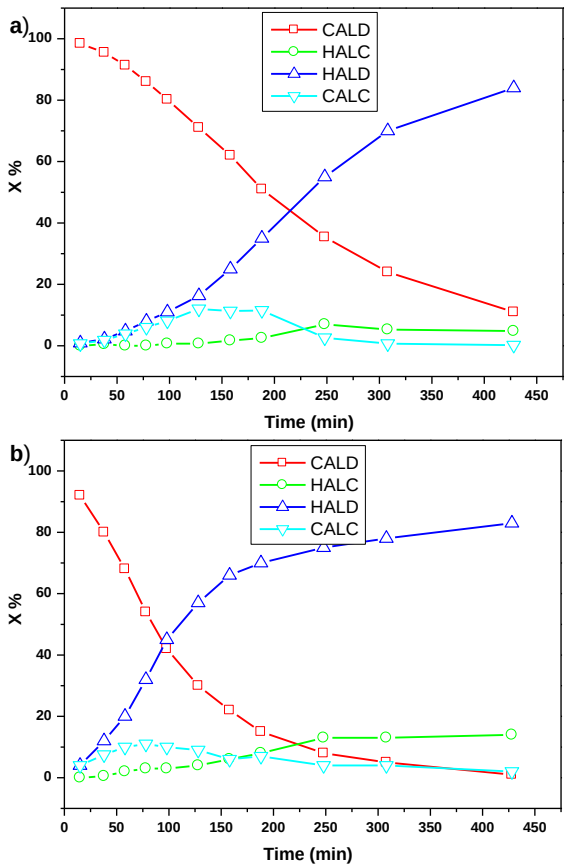

Fig. 7 Course of hydrogenation of CALD over a) Pd/TNT and b) Pd/STNT.

Table 3 Hydrogenation of CALD over various catalysts: mass reaction rate and product selectivity.

Catalyst	r (g_{CALD} g_{Pd}^{-1} h^{-1})	Selectivity (%)[b]		
		HALD	HALC	CALC
[a]Pd/C	48	87	12	<1
Pd/TNT	65	85	14	1
Pd/STNT^{1st}	151	84	15	1
Pd/STNT^{3rd}	137	82	16	2

[a]commercial Pd/C catalysts bought from Aladin agent company (Shanghai, China)

[b]Selectivity was determined at 80% CALD conversion; no other product was found in the GC-mass spectra.

4.Discussion

Based on the above results, we conclude that the introduced silane were transformed into silica, underwent the calcination at 400 ℃, and then were deposited on the surface of TNT(see Scheme 1). The effect of silica modification on the TNT can be seen as: resist crystallization (justified by the XRD and Raman spectra) and morphology collapse (justified by the TEM observation) during calcination. The decreased crystalline can be explained as that the SiO_2 lattice locked the Ti-O species at the

interface with the TiO_2 domains and prevented the nucleation that was necessary for the crystallization and phase transformation[41]. The lower crystalline degree means larger content of amorphous bulk for the STNT, which could strengthen the metal–support interaction[42]. With respect to the morphology collapse the deposited silica can act as "isolation wall" to retard the condensation of hydroxyl groups during calcination. There is a common agreement that the interlayer hydroxyl groups and water in the multi-walled structure of TNT act as support to maintain the tubular morphology[31]. As the tubular morphology is maintained intact, high surface area are well preserved, as shown by N_2 sorption in Table 1. In addition, the amorphous silica layer deposited on the surface of TNT could contribute to the high surface area as well.

When the Pd NPs were loaded on the modified STNT support, the metal dispersion (seeing TEM images of Fig. 3) and composition (atomic ratio of Pd^0/Pd^{II}, seeing XPS result of Table 2) of Pd NPs was greatly modulated. The improved metal dispersion can be ascribed to the high surface area of STNT. Plus, the strengthened Pd-support interaction, indicating by the shift of binding energy of Pd and Ti (seeing Fig. 4), could effectively hind the metal sintering, and decrease the particle size. Moreover, the charge transfer induced by the intensified Pd-support interaction can facilitate the reduction of Pd species and produce more metallic Pd phase. Some studies[13, 14] have proven that compositing TiO_2 with other metal oxides (e.g., SiO_2, Al_2O_3) can effectively modify the metal-support interactions. The improved H_2 adsorption capacities for the Pd/STNT catalysts (justified by the H_2-TPD) could be related to metal dispersion/composition strongly: (i) high metal dispersion creates more active sites for hydrogen adsorption; (ii) high metallic Pd content also facilitates H_2 adsorption. Much more active sites were produced, when silica-modified TNT was used as the support;one would expect this to result in enhanced catalyst performance.

Clearly, the catalytic performance of catalysts towards the hydrogenation of CALD (presented in Fig. 7) verified the above assumption. The great enhanced hydrogenation activity of Pd/STNT can be obviously ascribed to its high Pd dispersion, in one respect. Plus, the large surface of STNT could contribute to the improved activity due to the high external surface area could facilitate mass transfer. In another respect, it should be noticeably that the greater improvement shown by silica modification is associated with its ratio of Pd^0/Pd^{II}, indicating the important role of metallic Pd phase. In Winterbottom's early work[43], it has revealed that pre-reduced PdO gave rise to better activity for the liquid-phase hydrogenation of 1-octyne at 30 ℃, indicating that metallic Pd could accelerate the hydrogenation rate. Agostini's group[44] recently has declared that the metallic phase of Pd can shorten the induction period for the debenzylation process catalyzed by Pd/Al_2O_3. Thus, we hypothesize that the metallic phase can also preferentially promote hydrogenation activity, overwhelming the PdO phase at low temperatures (<30 ℃). This can come about in two ways: metallic Pd can (i) facilitate hydrogen dissociative adsorption and (ii) accelerate the induction period of hydrogenation. In a word, silica modification can change the Pd-TiO_2 interaction, yielding much more of the metallic Pd phase, increasing the active center sites for hydrogenation, and consequently improving the catalytic activity at low reaction temperatures.

5. Conclusions

We report high-performance Pd catalysts with silica modified TNT (STNT) as supports. The catalysts show improved performance towards the hydrogenation of cinnamaldehyde at ambient temperature. The effect of silica modification on the TNT support can be regard as resist crystallization and morphology collapse during calcination, change the interface structure and properties of TNT. The modified surface further modulates the Pd-support interaction strongly and cause high metal dispersion and metallic Pd content, both of which could enhance its hydrogenation activity significantly. Pd/STNT in particular may shed light on the design of promising catalysts for hydrogenation in green catalysis applications.

Notes and references

[a]*Key Laboratory of Renewable Energy, Guangzhou Institute of Energy Conversion, Chinese Academy of Sciences, Guangzhou, China; Tel: +86 02 87057371; E-mail: lixj@ms.giec.ac.cn*
[b]*School of Chemistry and Chemical Engineering, South China University of Technology, Guangzhou, China; Tel: +86 02 87113586; E-mail: chsjliao@scut.edu.cn*

This work was supported by the National Scientific Foundation of China (project no. 21303210), the National 973 Project of China (project no. 2009CB220002),and the Postdoctoral Foundation of China (project no. 2013M531881), the Fundamental Research Funds for the Central Universities, SCUT.

1. A. Fukuoka and P. L. Dhepe, *Chem. Rec.*, 2009, **9**, 224-235.
2. P. T. Anastas, L. B. Bartlett, M. M. Kirchhoff and T. C. Williamson, *Catal. Today*, 2000, **55**, 11-22.
3. V. Polshettiwar and R. S. Varma, *Green Chem.*, 2010, **12**, 743-754.
4. J. Mao, G. Zhao, D. Wang and Y. Li, *Rsc Adv.*, 2014, **4**, 25384-25388.
5. X. Peng, W. Ye, Y. Ding, S. Jiang, M. Hanif, X. Liao and H. Hou, *Rsc Adv.*, 2014, **4**, 42732-42736.
6. S. Rostamnia and E. Doustkhah, *Rsc Adv.*, 2014, **4**, 28238-28248.
7. J. Safari and S. Gandomi-Ravandi, *Rsc Adv.*, 2014, **4**, 11486-11492.
8. M. Yadav, D. K. Mishra and J.-S. Hwang, *Appl. Catal. A*, 2012, **425**, 110-116.
9. A. Villa, G. M. Veith, D. Ferri, A. Weidenkaff, K. A. Perry, S. Campisi and L. Prati, *Catal. Sci. Technol.*, 2013, **3**, 394-399.
10. J. Zhu, M. Li, M. Lu and J. Zhu, *Catal. Sci. Technol.*, 2013, **3**, 737-744.
11. N. Jagtap, S. B. Umbarkar, P. Miquel, P. Granger and M. K. Dongare, *Appl. Catal. B*, 2009, **90**, 416-425.
12. Z. Zhang, Y. Zhou, Y. Zhang, X. Sheng, S. Zhou and S. Xiang, *Rsc Adv.*, 2014, **4**, 40078-40084.
13. G. Wan, A. Duan, Z. Zhao, G. Jiang, D. Zhang, R. Li, T. Dou and K. H. Chung, *Energy Fuels*, 2008, **23**, 81-85.
14. W. Yan, S. M. Mahurin, Z. Pan, S. H. Overbury and S. Dai, *J. Am. Chem. Soc.*, 2005, **127**, 10480-10481.
15. X. Sun and Y. Li, *Chem. Euro. J.*, 2003, **9**, 2229-2238.
16. L. Torrente-Murciano, A. A. Lapkin, D. V. Bavykin, F. C. Walsh and K. Wilson, *J.Catal.*, 2007, **245**, 272-278.
17. M. Wang, D.-j. Guo and H.-l. Li, *J. Solid State Chem.*, 2005, **178**, 1996-2000.
18. V. Idakiev, Z.-Y. Yuan, T. Tabakova and B.-L. Su, *Appl. Catal. A*, 2005, **281**, 149-155.
19. D. V. Bavykin, A. A. Lapkin, P. K. Plucinski, L. Torrente-Murciano, J. M. Friedrich and F. C. Walsh, *Top. Catal.*, 2006, **39**, 151-160.

20. H.-H. Ou and S.-L. Lo, *Separation Purification Technol.*, 2007, **58**, 179-191.
21. S. H. Joo, J. Y. Park, C.-K. Tsung, Y. Yamada, P. Yang and G. A. Somorjai, *Nat. Mater.*, 2009, **8**, 126-131.
22. A. C. S. Sekhar, C. J. Meera, K. V. Ziyad, C. S. Gopinath and C. P. Vinod, *Catal. Sci. Technol.*, 2013, **3**, 1190-1193.
23. B. Zeng, B. Hou, L. Jia, J. Wang, C. Chen, D. Li and Y. Sun, *Catal. Sci. Technol.*, 2013, **3**, 3250-3255.
24. L. Mo, K. K. M. Leong and S. Kawi, *Catal. Sci. Technol.*, 2014, **4**, 2107-2114.
25. D. Li, D. Shi, Z. Liu, H. Liu and Z. Guo, *J. Nanoparticle Res.*, 2013, **15**, 1-10.
26. K. Okada, N. Yamamoto, Y. Kameshima, A. Yasumori and K. J. MacKenzie, *J. Am. Ceramic Soc.*, 2001, **84**, 1591-1596.
27. S. Tauster, S. Fung and R. Garten, *J. Am. Chem. Soc.*, 1978, **100**, 170-175.
28. H. Chen, Y. Shao, Z. Xu, H. Wan, Y. Wan, S. Zheng and D. Zhu, *Appl. Catal. B*, 2011, **105**, 255-262.
29. T. Gao, H. Fjellvåg and P. Norby, *Inorg. Chem.*, 2009, **48**, 1423-1432.
30. F. Tian, Y. Zhang, J. Zhang and C. Pan, *J. Phys. Chem. C*, 2012, **116**, 7515-7519.
31. E. Morgado Jr, M. A. S. de Abreu, O. R. C. Pravia, B. A. Marinkovic, P. M. Jardim, F. C. Rizzo and A. S. Araújo, *Solid State Sci.*, 2006, **8**, 888-900.
32. R. Yoshida, Y. Suzuki and S. Yoshikawa, *Mater. Chem. Phys.*, 2005, **91**, 409-416.
33. J. Yu, H. Yu, B. Cheng and C. Trapalis, *J. Mol. Catal. A*, 2006, **249**, 135-142.
34. A. Binder, M. Seipenbusch and G. Kasper, *J. Phys. Chem. C*, 2010, **114**, 7816-7821.
35. G. Zhang, Y. Wang, X. Wang, Y. Chen, Y. Zhou, Y. Tang, L. Lu, J. Bao and T. Lu, *Appl. Catal. B*, 2011, **102**, 614-619.
36. X. Yang, D. Chen, S. Liao, H. Song, Y. Li, Z. Fu and Y. Su, *J. Catal.*, 2012, **291**, 36-43.
37. H. Zhu, Z. Qin, W. Shan, W. Shen and J. Wang, *J. Catal.*, 2004, **225**, 267-277.
38. D. Xu, W. Li, H. Duan, Q. Ge and H. Xu, *Catal. Lett.*, 2005, **102**, 229-235.
39. A. Mehri, H. Kochkar, S. Daniele, V. Mendez, A. Ghorbel and G. Berhault, *J. Colloid Interface Sci.*, 2012, **369**, 309-316.
40. Y. J. Zhu and F. Zaera, *Catal. Sci. Technol.*, 2014, **4**, 955-962.
41. Z. Li, B. Hou, Y. Xu, D. Wu and Y. Sun, *J. Colloid Interface Sci.*, 2005, **288**, 149-154.
42. J. Panpranot, K. Kontapakdee and P. Praserthdam, *J. Phys. Chem. B*, 2006, **110**, 8019-8024.
43. I. Caga, E. Shutt and J. Winterbottom, *J. Catal.*, 1976, **44**, 271-280.
44. E. Groppo, G. Agostini, A. Piovano, N. B. Muddada, G. Leofanti, R. Pellegrini, G. Portale, A. Longo and C. Lamberti, *J. Catal.*, 2012, **287**, 44-54.